SAND2008-4306P

Aerodynamic and Aeroacoustic Properties of a Flatback Airfoil (Will it Rumble or Whisper?)

Dale E. Berg* and Matthew Barone†
Sandia National Laboratories‡
Albuquerque, NM 87185-1124 USA

Abstract:

The blade design resulting from the Sandia National Laboratories (SNL) Blade Systems Design Study, known as the BSDS blade, utilizes "flatback" airfoils for the inboard section of the blade to achieve a lighter, stronger blade. Compared to a thick conventional, sharp trailing-edge airfoil, a flatback airfoil with the same thickness exhibits increased lift and reduced sensitivity to soiling. In order to quantify the aerodynamic and noise generation characteristics of flatback airfoils, Sandia National Laboratories has conducted a wind tunnel test to measure the noise generation and aerodynamic performance characteristics of a regular DU97-W-300 airfoil, a 10% trailing edge thickness flatback version of that airfoil, and the flatback fitted with a trailing edge treatment. Limited results from the test are presented. The flatback generates considerably more sound than the sharp trailing edge airfoil, but that sound is significantly reduced by the addition of a simple splitter plate to the flatback trailing edge. The data are shown to be consistent with prior aerodynamic tests on the sharp trailing edge configuration and with prior aeroacoustic tests on blunt trailing edge airfoils.

I. Introduction

In 2002, the Wind Energy Technology Department of Sandia National Laboratories (SNL) initiated a research program to demonstrate the use of carbon fiber in wind turbine blades and to investigate advanced structural concepts through the Blade Systems Design Study, known as the BSDS. One of the blade designs resulting from this program, commonly referred to as the BSDS blade (shown in Figure 1), resulted from a systems approach in which manufacturing, structural and aerodynamic performance considerations were all simultaneously included in the design optimization. Berry[1] discusses the design of this blade in some detail. The system design approach led the designers of the BSDS to utilize flatback airfoils for the inboard portion of the blade. The full thickness of the flatback tapers from its maximum near the blade root to a conventional, sharp trailing edge somewhere inboard of 40% of blade span. Flatback airfoils are generated by opening up the trailing edge of the airfoil uniformly along the camber line, as shown in Figure 2, thus preserving the camber of the original airfoil. This is in distinct contrast to truncated airfoils where the trailing edge of the airfoil is simply cut off, changing the camber and degrading the aerodynamic performance. Compared to thick conventional, sharp trailing-edge wind turbine airfoil, such as those designed by Delft[2,3] or Riso[4], a flatback airfoil with the same thickness exhibits increased lift and reduced sensitivity to soiling, according to Standish[5]. In addition, the use of flatback airfoils permits the use of increased thickness airfoils without the chord increases that would occur if conventional thick airfoils were used. Avoiding this additional chord length makes the resulting structural design simpler and easier to build, resulting in a blade that is easier to transport.

---

* Principal Member of Technical Staff, Wind Energy Technology Department, MS-1124
† Senior Member of Technical Staff, Wind Energy Technology Department, MS-1124
‡ Sandia is a multiprogram laboratory operated by Sandia Corporation, a Lockheed Martin Company, for the United States Department of Energy's National Nuclear Security Administration under contract DE-AC04-94AL85000.

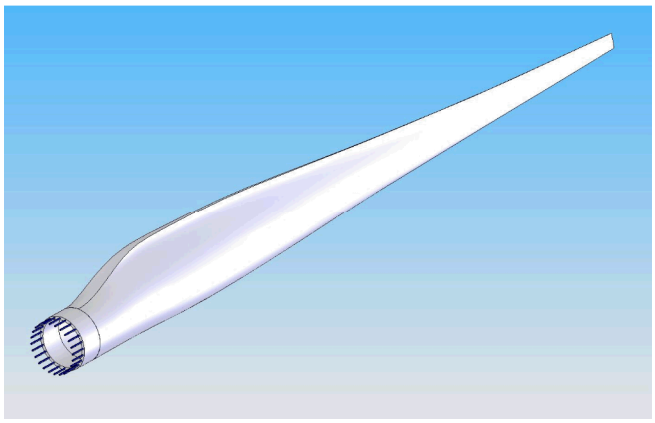

Figure 1: The BSDS rotor blade incorporating a flatback airfoil. Notice that the flat trailing edge near the root tapers to a sharp trailing edge by 40% of span.

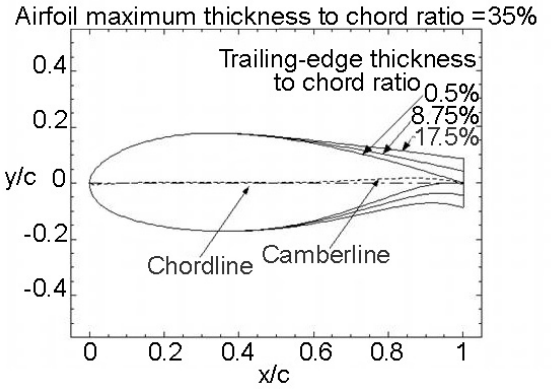

Figure 2: Flatback airfoil

These benefits do not come without risks, however, as there may be issues and concerns associated with aeroacoustics, excess drag, and three-dimensional flow along the trailing edge. The issue of acoustic emission from the flatback airfoils should be mitigated by their inboard location, where airspeeds are low. Given that these airfoils are designed for use on the inner portion of the blade ($r/R<0.5$) and sound intensity scales as V^5 (due to the interaction of a turbulent boundary layer with a sharp trailing edge), according to Brooks, Pope and Marcolini[6], any noise produced will be attenuated by at least a factor of $2^5(=32)$ compared to noise produced at the tip. Brooks, *et al*[6] do present an empirical relationship for estimating the effects of trailing edge thickness (called "bluntness" by Brooks, *et al*) on noise generation, but the maximum degree of trailing edge thickness for which they have data is approximately 1% of chord; an order of magnitude lower than what is apt to be encountered with the use of flatback airfoils.

Previous work has demonstrated that utilizing flatback airfoils in the root area of a wind turbine blade can result in decreases in blade weight and cost, both critical issues for the next generation of wind turbine blades[7]. Several commercial turbine manufacturers have expressed interest in utilizing flatback airfoils for their wind turbine blades designs, but they are always very concerned about the potential extra noise that such a blade will generate from the blunt trailing edge of the flatback section. Existing analytical tools are not capable of accurately predicting the magnitude or character of this noise.

In order to quantify the noise generation and aerodynamic performance characteristics of flatback airfoils, Sandia National Laboratories has conducted a wind tunnel test to compare the noise generation of a regular DU97-W-300 airfoil[2,3], a 10% trailing edge thickness flatback version of that airfoil, and the flatback modified by the addition of a trailing edge splitter plate. A previous paper has described the test facility, the models, and the test methodology, and provided some preliminary results from the test[8]. This paper will present a snapshot of some of the aerodynamic and aeroacoustic results from that test.

II. Test Facility, Models and Test Methodology

The Virginia Tech wind tunnel used in this work was recently extensively modified for performing aeroacoustic tests. Carmargo, Smith, Devenport and Burdisso[9] explain how the original walls of the test section were replaced with tensioned sheets of woven Kevlar, which allow sound to pass through with very little attenuation, but largely confine the air flow in the tunnel. Anechoic chambers are located behind each of the Kevlar windows to fully confine the flow and provide space for mounting acoustic measuring equipment. Carmargo *et al*[9] also describe the extensive calibration that was performed on the tunnel to confirm that the modification did not degrade the original high quality flow. Ongoing efforts

continue to quiet the tunnel and thus permit more accurate measurements of the noise produced by test airfoils.

The facility is capable of acquiring aerodynamic loads on the test airfoil (through the use of airfoil surface pressure ports and a wake rake), detailed hot-wire measurements in the trailing edge boundary layer and detailed acoustic source data (via use of a 63 microphone phased array).

The two airfoil models used in this test were fabricated by Novakinetics, Inc. of Flagstaff, AZ. Both were 0.91 m (36 in) in chord and 1.83 m (6 ft) in span. The nominally sharp trailing edge is 1.6 cm (0.625 in) thick, and the 10% flatback trailing edge is 9.1 cm (3.6 in) thick. Figure 3 is a photograph of the cross section of the flatback model. A third configuration resulted from attaching a splitter plate, with length equal to the trailing edge thickness, to the flatback trailing edge surface, halfway between the upper and lower airfoil surfaces. Figure 4 is a photograph of the flatback model with the splitter plate attached. Measurements have confirmed that the model shapes conform closely to the design drawings.

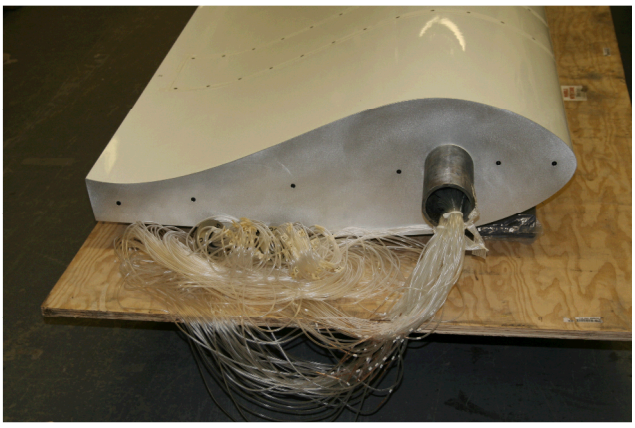

Figure 3: Flatback wind tunnel model.

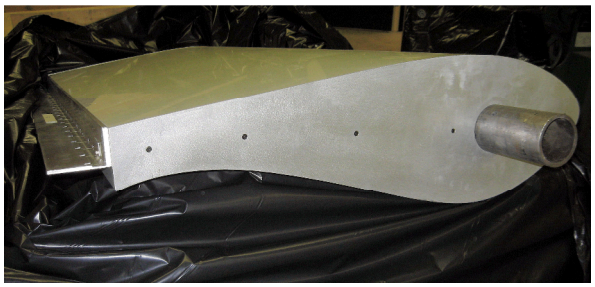

Figure 4: Flatback wind tunnel model with Splitter plate attached.

The models were inserted through the floor of the test section and were mounted vertically, as illustrated in Figure 5. Model angle of attack was adjusted for tunnel blockage effects and was set manually.

All measurements were obtained with the airfoil stationary. The model angle of attack was set, the tunnel operating speed was brought up to the appropriate levels for the Reynolds numbers of interest and the required measurements were obtained at each Reynolds number. The tunnel speed was then brought down to nearly zero, the angle of attack was changed and the procedure was repeated.

Although the wind tunnel is capable of operating at Reynolds numbers (based on model chord) as high as about 5×10^6 for this size model, concern about the effect of extreme velocities on the Kevlar acoustic windows (especially with the vortex shedding that was expected from the flatback airfoil) limited the maximum nominal Reynolds numbers for this test to 3.2×10^6. Tests were also conducted a lower nominal Reynolds numbers of 1.6×10^6 and 2.4×10^6 in order to evaluate the scaling of noise generation with flow velocity.

Figure 5: DU97-W-300 model in wind tunnel test section. View is upstream.

The pressures from the model surface taps were measured with a Scanivalve system. Wake pressures were measured with a single Pitot static probe mounted on a traversing mechanism near the airfoils mid span. All pressure measurements were 1-second averages of data acquired at 1000 Hertz.

Data acquired for the aeroacoustic characterizations included microphone phased-array data, hot-wire traverses of the airfoil boundary layers, both just upstream and just downstream of the trailing edge, and a limited amount of hot-wire spectral data. The acquisition of hot wire data near the surface of the flatback airfoil proved to be especially difficult – the extremely turbulent wake generated high loads on the probe support, resulting in large-amplitude probe tip vibration. This vibration, in turn, resulted in impacts of the tip on the model and subsequent breakage of the hot wire.

The microphone phased array, shown in Figure 6 was located in the anechoic chamber on the right side of the test chamber (looking upstream), with the plane of the array vertical and parallel to the test section center line. The array consisted of 63 microphones; 9 microphones located along each of 7 arms. All 63 microphones are sampled simultaneously at 25,600 Hz to acquire close to one million samples for each microphone for each combination of test configuration and tunnel condition. Figure 7 illustrates the location and orientation of the phased array relative to the airfoil model. The signals within a specified frequency band from all the microphones are compared and combined with the delay times required for sound from a potential source to reach each of the microphones to identify the actual location of each sound source. This process is typically known as "beam forming". The resolution of this technique is pretty poor below 500 Hz, so no data are acquired or reduced at frequencies below that level.

Data were obtained for both smooth airfoil and boundary layer trip configurations, referred to subsequently as "clean" and "tripped" conditions. The boundary layer trip consisted of 5 mm wide, 0.5 mm thick zig-zag serrated tape running the entire span of the model, placed at 5% chord on the suction side of the model and at 10% chord on the pressure side of the model.

The test goal was to acquire both aeroacoustic and aerodynamic data for all three model configurations at the three Reynolds numbers mentioned above, at several angles of attack ranging from just below C_{dmin} to just above C_{lmax} (as predicted by a CFD code) for both clean and tripped conditions. Time constraints precluded obtaining complete data at all of these conditions.

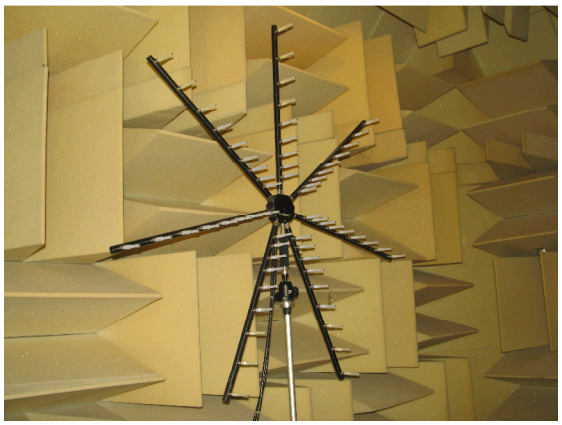

Figure 6: Microphone phased array.

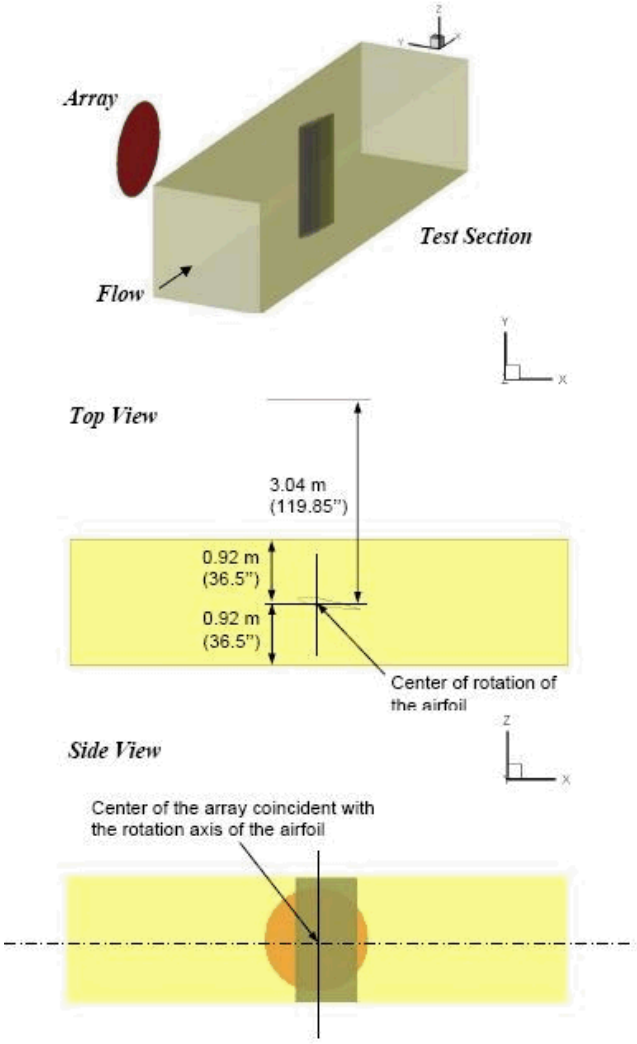

Figure 7: Location of phased array in the wind tunnel.

III. Aerodynamic Performance

Initial reduction of the sharp trailing edge pressure data applying a wind-tunnel wall downwash correction yielded lift data that differed significantly from data that was obtained on a similar airfoil by researchers at the Technical University of Delft (TU Delft)[2]. As an initial step to resolve this ambiguity, Virginia Tech ran the sharp model in the solid wall test section in May 2008. Figure 8 shows the lift and moment coefficients for the sharp trailing edge airfoil for three separate wind tunnel tests: the current test in the stability tunnel with Kevlar test section walls; the check runs in the same tunnel with solid test section walls; and a test performed in the low-speed, low-turbulence, solid-wall wind tunnel at TU Delft. The Kevlar test section data were corrected for upwash by comparing measured pressure distributions with predictions from a linear panel-method code, and estimating an effective angle of attack for the measured conditions. This method does not account for model blockage effects or for possible non-linear porous wall boundary effects, and the results do not agree with the two solid wall tests. The solid wall data is corrected for wall interference and blockage. The results of the two solid wall tests agree well with one another. Solid wall pressure distributions (corrected for blockage) at $\alpha = 4$ and 8 degrees, shown in

Figure 9, also agree well between the two tests, giving confidence in the measurement systems of the present test and indicating that more detailed wind tunnel wall corrections are needed for the Kevlar test section aerodynamic data. Measurements of the wall porosity and vortex panel/CFD calculations will be used to determine the porous wall test section corrections for the sharp trailing edge airfoil, and these corrections will be used to reduce the aerodynamic data for the other two model configurations.

Baker, van Dam and Gilbert[10] found that the splitter plate decreased the C_{lmax} of the flatback airfoil by a small amount, with very little impact on the lift-curve slope and reduced the drag of the flatback airfoil by about 50% at a Reynolds number of 333,000. Similar effects are anticipated for this test.

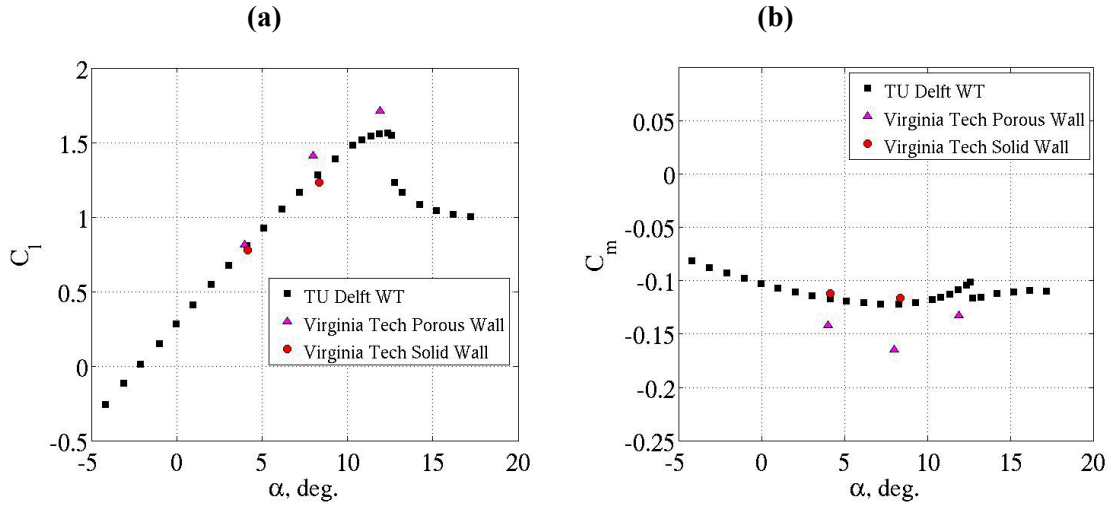

Figure 8: Sharp trailing edge airfoil aerodynamic coefficients.

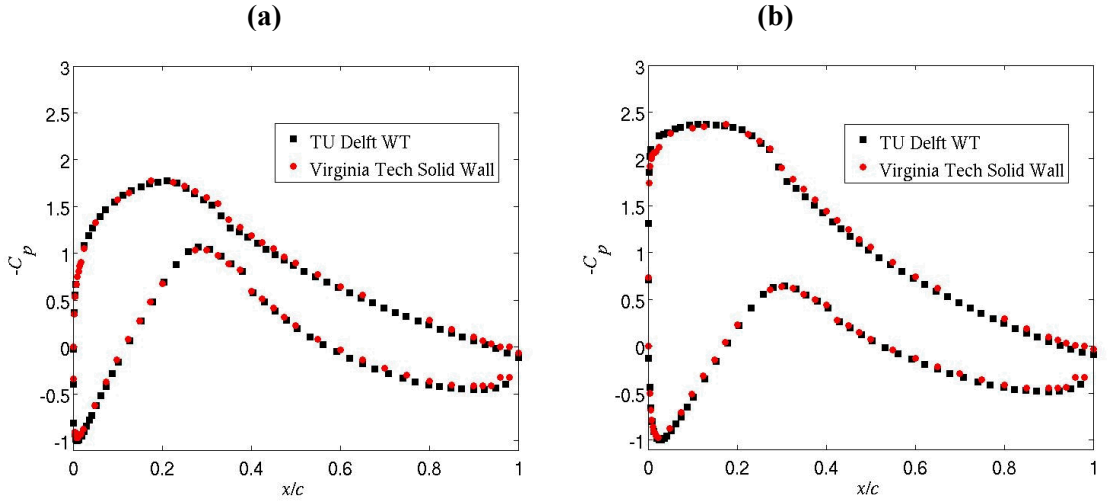

Figure 9: Sharp trailing edge airfoil pressure distributions. (a) α= 4 degrees. (b) α= 8 degrees.

IV. Aeroacoustic Results

The noise spectra below 500 Hz that result from performing FFT operations on the acoustic array data were averaged to determine a mean spectrum for each microphone in the array. These were merged with

the beam-formed spectra for frequencies above 500 Hz to yield the sound spectra presented in Figure 10. The integration of these spectra yields the actual perceived sound generated by the airfoil. The DU97-W-300 data is somewhat questionable, since it is nearly masked by the ambient wind tunnel sound. The sound pressure levels of the three configurations are 77 dB for the sharp trailing edge configuration, 100 dB for the flatback configuration and 88 dB for the flatback with splitter plate configuration. From Figure 10 it is obvious that the flatback configuration generates much, much more sound than the DU97-W-300 airfoil, especially in the 100-200 Hz frequency band. The splitter plate decreases the sound level significantly in the 100-200 Hz frequency range and to a much reduced extent over the entire frequency range above 200 Hz. However, the sound level for the flatback with splitter plate is still well above the DU97-W-300 airfoil level in the 100-200 Hz band.

The large peak for the flatback airfoil in Figure 10 at about 150 Hz is due to the vortex shedding at that frequency. Addition of the splitter plate causes the reduction of that particular peak and creation of a second, somewhat higher, shedding frequency.

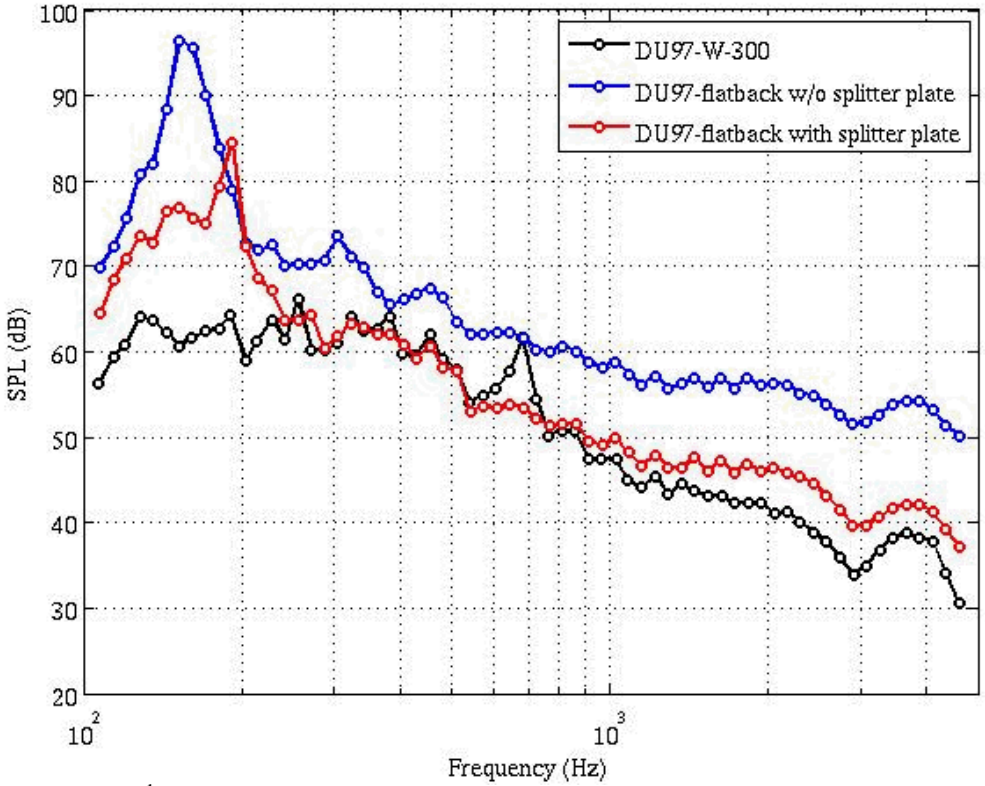

Figure 10: 1/12th octave band spectra for the three airfoil configurations at a=4 degrees, clean, Re = 3 million.

The qualitative manner in which the splitter plate interacts with the flow field to cause this reduction in sound level is illustrated in Figures 11 and 12, which illustrate the flow fields about these configurations, as determined by two-dimensional CFD simulations. These calculations assumed fully turbulent flow and utilized the Detached Eddy Simulation hybrid turbulence model. In Figure 11, large-scale, very coherent vortices are observed being shed. The addition of the splitter plate in Figure 12 results in almost complete disappearance of those coherent vortices close to the trailing edge. Smaller scale vortices are still visible, but they create far less sound, and their smaller length and time scales result in higher-frequency sound.

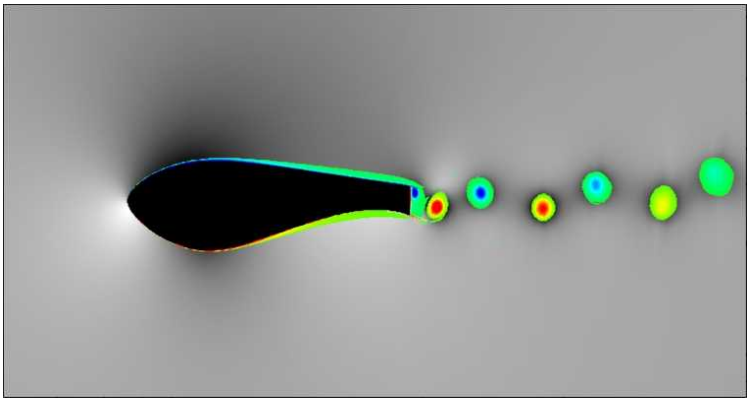

Figure 11: CFD simulation of vorticity shedding for the flatback airfoil at Re=3X10^6 and α=4 degrees.

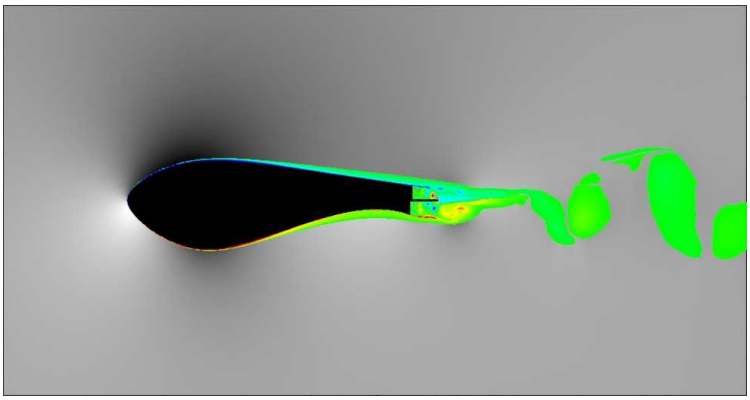

Figure 12: CFD simulation of **v**orticity shedding for the flatback airfoil with splitter plate at Re=3X10^6 and α=4 degrees.

The Strouhal number ($St = \frac{fh}{V}$, where f is the shedding frequency, h is the height of the flatback, and V is the local velocity) of the vortex-shedding tone for the flatback airfoil with and without the splitter plate attached is plotted versus chord Reynolds number in Figure 13. Also plotted are the results reported by Bearman[11] for a blunt trailing edge body with zero trailing edge angle, an elliptical leading edge, and a ratio of base height to boundary layer displacement thickness of $h/\delta^* \approx 10$. Bearman also made measurements with a splitter plate with length equal to the trailing edge base height in a configuration very similar to the present experiment. The empirical correlation of Brooks, et al[6] is also shown in the plot for the geometry and flow conditions of Bearman, and for the present flatback configuration where $h/\delta^* \approx 19$ and the trailing edge included angle is -11 degrees (divergent trailing edge angle). The Brooks correlation under-predicts the Bearman data, since for large h/δ^* and zero trailing edge angle the correlation asymptotes to St = 0.21. The correction for negative included trailing edge angle gives good agreement of the correlation with the flatback data; however, it should be noted that this is an extrapolation of the correlation, since the data-set upon which the correlation is based does not include any divergent trailing edge data. Focusing on the flatback results, the Strouhal number is relatively insensitive to Reynolds number, angle of attack, and whether the boundary layer is tripped or not over the range of experimental conditions. The addition of a splitter plate uniformly raises the Strouhal number of the peak shedding frequency, in accordance with Bearman's results, and seems to accentuate the effect of the boundary layer trip for α = 10 degrees.

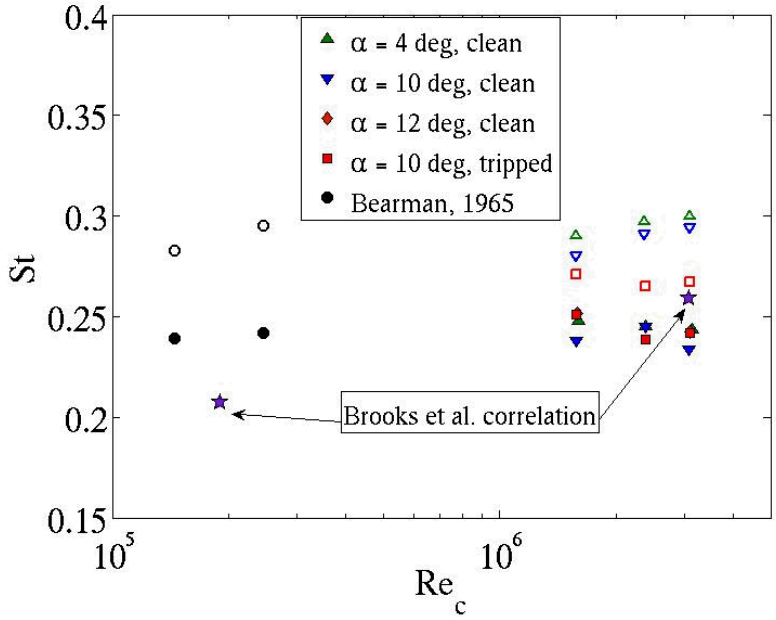

Figure 13: Vortex-shedding Strouhal number versus chord Reynolds number for the flatback airfoil, compared with previous data. Open/Closed symbols are with/without the splitter plate attached.

Figure 14 shows the broadband trailing edge noise sound pressure level for $f \geq 2f_0$, where f_0 is the fundamental vortex shedding frequency (75, 112.5, and 150 Hz for free stream velocities of 28, 43 and 57 m/s, respectively), for the clean flatback model at $\alpha = 4$ degrees, plotted versus free-stream velocity. This frequency range is the range over which the beam-forming algorithm was successful in isolating the trailing edge noise, and for which the wind tunnel chamber is anechoic for each flow condition. It does not include the primary vortex-shedding tone, which occurred in the range $75 \leq f \leq 150$ Hz. Assuming that the sound source mechanism does not depend on Reynolds number, aeroacoustic theory predicts that the intensity of a compact sound source with acoustic wavelength much larger than airfoil chord will scale with the sixth power of the flow velocity, while intensity of high-frequency sound with wavelength much shorter than the airfoil chord scales with the fifth power of the flow velocity. The expected scaling should lie somewhere between these limits. As seen in the figure, the two higher flow velocity measurements are very close to obeying the fifth power scaling, while the two lowest flow velocity measurements are close to the sixth power scaling. This behavior is consistent with the aeroacoustic theory, since larger flow velocities are associated with higher frequency sound.

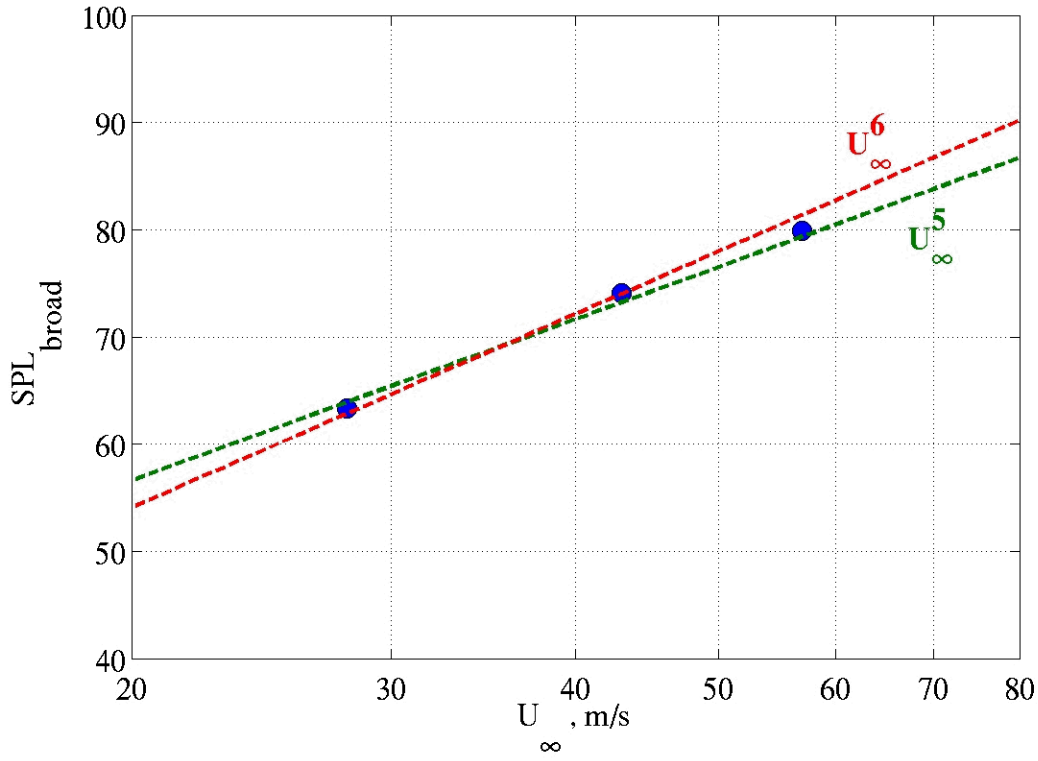

Figure 14: Dependence of high-frequency broadband SPL on flow on flow velocity, clean flatback airfoil at $\alpha = 4$ degrees.

V. Future Direction

Now that we have the models, it would be fairly simple (all we need is funding) to run additional tests on the current configurations to fill out the measurement matrix with additional data at existing angles of attack and add more angles of attack. We are also considering looking at other splitter plate configurations to see if any are more effective at reducing noise generation.

Careful examination of the acoustic data has revealed that the sound reflection and cancellation characteristics of the wind tunnel have probably contaminated the acoustic data in the 100 to 500 Hz frequency range, compromising the measurement accuracy of the sound generated by vortex shedding from the flatback trailing edge. Current plans call for additional testing to characterize the acoustic properties of the tunnel at these low frequencies.

VI. Summary

Wind tunnel tests were conducted at nearly full-scale Reynolds number conditions to directly compare the aerodynamics and aeroacoustic performance of conventional and flatback airfoils designed for use in the root section of a wind turbine rotor. The effect on noise generation and aerodynamic performance of adding a simple trailing edge splitter plate to the flatback airfoil were also determined. Data obtained in the tests included surface and wake pressure measurements, hotwire boundary layer surveys and microphone phased array acoustic data. Data were obtained at Reynolds numbers, based on chord length,

of approximately 1.6 X 10^6, 2.4 X 10^6 and 3.2 X 10^6, for angles of attack from 4° to 12°, both with a clean airfoil surface and with tripped boundary layers.

Simulations of sharp trailing edge aerodynamic performance with a conventional CFD code, utilizing the Spalart-Allmares turbulence model, did not correlate well with the experimental data obtained in the Kevlar wall test section. Additional tests with a solid wall test section revealed good correlation with previous wind tunnel results for that airfoil, indicating that the porous wall corrections are inadequate. Efforts are now underway to determine the appropriate corrections.

The acoustics data show that, as expected, the flatback airfoil generates far more noise at these Reynolds numbers than does a conventional, sharp trailing edge airfoil. The addition of a simple trailing edge splitter plate reduced the intensity of the sound generated by the flatback airfoil from 100 dB to 88 dB (compared to 77 dB for the sound generated by a sharp trailing edge airfoil).

Detailed analysis of the sound data revealed that the acoustic characteristics of the tunnel have probably contaminated the acoustic data in the frequency range at which vortex shedding occurs. Additional testing to characterize that contamination is planned.

VII. Acknowledgements

The authors gratefully acknowledge the contributions of those at Virginia Polytechnic Institute and State University who actually ran the test, performed the data reduction and wrote the test report. They include Professors William Devenport (Director of the Stability Wind Tunnel) amd Ricardo Burdisso and their graduate students H. Camargo, Erin Crede, M. Remillieus, M. Rasnick and P. van Seeters.

VIII. References

1. Berry, D., 2007, *BSDS-II Final Project Report*, (Currently in review), Sandia National Laboratories, Albuquerque, NM.
2. Timmer, W.A., and van Rooij, R.P.J.O.M., 2003, *Summary of the Delft University Wind Turbine Dedicated Airfoils*, J. Solar Energy Engineering, Vol. 125, Nov. 2003, pp. 488-496.
3. van Rooij, R.P.J.O.M., and Timmer, W. A., 2003, *Roughness Sensitivity Considerations for Thick Rotor Blade Airfoils*, J. Solar Energy Engineering, Vol. 125, Nov. 2003, pp. 468-478.
4. Fuglsag, P, Bak, C., Gaunaa, M. and Antoniou, I., 2004, *Design and Verification of the Riso-B1 Airfoil Family for Wind Turbines*, J. Solar Energy Engineering, Vol. 126, Nov. 2004, pp. 1002-1010.
5. Standish, K. J., 2003, *Aerodynamic Analysis of Blunt Trailing Edge Airfoils & A Microtab-Based Load Control System*, M.S. Thesis, University of California, Davis, CA.
6. Brooks, T. F.; Pope, D. S.; and Marcolini, M. A., 1989. *Airfoil Self-noise and Prediction*, NASA RP 1218.
7. Paquette, J.A. and Veers, P.S, 2007, *Increased Strength in Wind Turbine Blades through Innovative Structural Design,* European Wind Energy Conference, Milan, Italy.
8. Berg, D. E., and Zayas, J. R., 2008, *Aerodynamic and Aeroacoustic Properties of Flatback Airfoils,* Proceedings, ASME/AIAA Wind Energy Symposium, Reno, NV, 2008.
9. Carmargo, H.E., Smith, B. S., Devenport, W.J., and Burdisso, R.A., 2005,"Evaluation and Calibration of a Prototype Acoustic Test Section for the Virginia Tech Stability Wind Tunnel", Report VPI=OAE-294, Virginia Polytechnic Institute and State University, May 2005.
10. Baker, J. P., van Dam, C. P., and Gilbert, B. L., 2008, *Flatback Airfoil Wind Tunnel Experiment*, SAND2008-2008, Sandia National Laboratories, Albuquerque, NM.

11. Bearman, P. W., 1965, *Investigation of the Flow Behind a Two-Dimensional Model with a Blunt Trailing Edge and Fitted with Splitter plates*, J. Fluid Mechanics, vol 21, part 2, pp. 241-255.